JOURNAL OF Applied Polymer SCIENCE

Special Issue: Manufacturing of Advanced Biodegradable Polymeric Components

Guest Editors: Prof. Roberto Pantani (University of Salerno) and
Prof. Lih-Sheng Turng (University of Wisconsin–Madison)

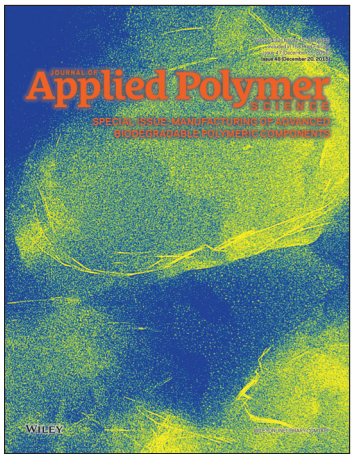

EDITORIAL

Manufacturing of advanced biodegradable polymeric components
R. Pantani and L.-S. Turng, *J. Appl. Polym. Sci.* 2015, **DOI: 10.1002/app.42889**

REVIEWS

Heat resistance of new biobased polymeric materials, focusing on starch, cellulose, PLA, and PHA
N. Peelman, P. Ragaert, K. Ragaert, B. De Meulenaer, F. Devlieghere and Ludwig Cardon, *J. Appl. Polym. Sci.* 2015, **DOI: 10.1002/app.42305**

Recent advances and migration issues in biodegradable polymers from renewable sources for food packaging
P. Scarfato, L. Di Maio and L. Incarnato, *J. Appl. Polym. Sci.* 2015, **DOI: 10.1002/app.42597**

3D bioprinting of photocrosslinkable hydrogel constructs
R. F. Pereira and P. J. Bartolo, *J. Appl. Polym. Sci.* 2015, **DOI: 10.1002/app.42458**

ARTICLES

Largely toughening biodegradable poly(lactic acid)/thermoplastic polyurethane blends by adding MDI
F. Zhao, H.-X. Huang and S.-D. Zhang, *J. Appl. Polym. Sci.* 2015, **DOI: 10.1002/app.42511**

Solubility factors as screening tools of biodegradable toughening agents of polylactide
A. Ruellan, A. Guinault, C. Sollogoub, V. Ducruet and S. Domenek, *J. Appl. Polym. Sci.* 2015, **DOI: 10.1002/app.42476**

Current progress in the production of PLA–ZnO nanocomposites: Beneficial effects of chain extender addition on key properties
M. Murariu, Y. Paint, O. Murariu, J.-M. Raquez, L. Bonnaud and P. Dubois, *J. Appl. Polym. Sci.* 2015, **DOI: 10.1002/app.42480**

Oriented polyvinyl alcohol films using short cellulose nanofibrils as a reinforcement
J. Peng, T. Ellingham, R. Sabo, C. M. Clemons and L.-S. Turng, *J. Appl. Polym. Sci.* 2015, **DOI: 10.1002/app.42283**

Biorenewable polymer composites from tall oil-based polyamide and lignin-cellulose fiber
K. Liu, S. A. Madbouly, J. A. Schrader, M. R. Kessler, D. Grewell and W. R. Graves, *J. Appl. Polym. Sci.* 2015, **DOI: 10.1002/app.42592**

Dual effect of chemical modification and polymer precoating of flax fibers on the properties of the short flax fiber/poly(lactic acid) composites
M. Kodal, Z. D. Topuk and G. Ozkoc, *J. Appl. Polym. Sci.* 2015, **DOI: 10.1002/app.42564**

Effect of processing techniques on the 3D microstructure of poly (L-lactic acid) scaffolds reinforced with wool keratin from different sources
D. Puglia, R. Ceccolini, E. Fortunati, I. Armentano, F. Morena, S. Martino, A. Aluigi, L. Torre and J. M. Kenny, *J. Appl. Polym. Sci.* 2015, **DOI: 10.1002/app.42890**

Batch foaming poly(vinyl alcohol)/microfibrillated cellulose composites with CO_2 and water as co-blowing agents
N. Zhao, C. Zhu, L. H. Mark, C. B. Park and Q. Li, *J. Appl. Polym. Sci.* 2015, **DOI: 10.1002/app.42551**

Foaming behavior of biobased blends based on thermoplastic gelatin and poly(butylene succinate)
M. Oliviero, L. Sorrentino, L. Cafiero, B. Galzerano, A. Sorrentino and S. Iannace, *J. Appl. Polym. Sci.* 2015, **DOI: 10.1002/app.42704**

Reactive extrusion effects on rheological and mechanical properties of poly(lactic acid)/poly[(butylene succinate)-*co*-adipate]/epoxy chain extender blends and clay nanocomposites
A. Mirzadeh, H. Ghasemi, F. Mahrous and M. R. Kamal, *J. Appl. Polym. Sci.* 2015, **DOI: 10.1002/app.42664**

JOURNAL OF Applied Polymer SCIENCE

Special Issue: Manufacturing of Advanced Biodegradable Polymeric Components

Guest Editors: Prof. Roberto Pantani (University of Salerno) and Prof. Lih-Sheng Turng (University of Wisconsin–Madison)

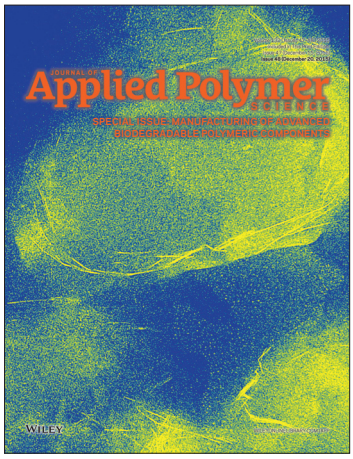

Rotational molding of biodegradable composites obtained with PLA reinforced by the wooden backbone of opuntia ficus indica cladodes
A. Greco and A. Maffezzoli, *J. Appl. Polym. Sci.* 2015, **DOI:** 10.1002/app.42447

Foam injection molding of poly(lactic) acid: Effect of back pressure on morphology and mechanical properties
V. Volpe and R. Pantani, *J. Appl. Polym. Sci.* 2015, **DOI:** 10.1002/app.42612

Modification and extrusion coating of polylactic acid films
H.-Y. Cheng, Y.-J. Yang, S.-C. Li, J.-Y. Hong and G.-W. Jang, *J. Appl. Polym. Sci.* 2015, **DOI:** 10.1002/app.42472

Processing and properties of biodegradable compounds based on aliphatic polyesters
M. R. Nobile, P. Cerruti, M. Malinconico and R. Pantani, *J. Appl. Polym. Sci.* 2015, **DOI:** 10.1002/app.42481

Journal of Applied Polymer Science

Foam injection molding of poly(lactic) acid: Effect of back pressure on morphology and mechanical properties

Valentina Volpe, Roberto Pantani
Department of Industrial Engineering, University of Salerno, Italy
Correspondence to: V. Volpe (E-mail: vavolpe@unisa.it)

ABSTRACT: Foam injection molding is a processing technology applied to produce a plastic part of a well-defined shape, containing a significant fraction of voids and thus consuming less material without sacrificing mechanical properties. This technology is particularly interesting for biodegradable polymers and in particular for poly(lactic acid), PLA, since it can be adopted to save material and to avoid thermal degradation due to its high viscosity at high shear rates, which requires high temperatures in traditional injection molding process. In this work a traditional injection molding machine, modified just in the cylinder to allow the gas injection, was adopted to obtain foam injection molding of a PLA grade. In particular, the effect of back pressure on foaming was assessed. Back pressure is the pressure imposed at the back of the screw when it is returning back to prepare a new amount of material to be injected (batching phase) and thus is particularly relevant in the formation of the polymer−gas mixture. It was shown that on increasing the back pressure the percentage of foaming agent inside the injection chamber is smaller, and thus foaming is less effective. The obtained samples were characterized as far as density and mechanical properties are concerned and it was found that it was possible to reduce the density of about 25% without a significant loss of mechanical properties. © 2015 Wiley Periodicals, Inc. J. Appl. Polym. Sci. **2015**, *132*, 42612.

KEYWORDS: biodegradable; foams; mechanical properties; morphology

Received 4 March 2015; accepted 15 June 2015
DOI: 10.1002/app.42612

INTRODUCTION

Foam injection molding is a processing technology in which a variant of the more traditional injection molding process is applied to produce a plastic part of a well-defined shape, consuming less material without sacrificing mechanical properties. The saving of material is achieved by creating voids by means of a foaming agent. In the "low pressure" version of foam injection molding, a controlled melt solution (plastic and blowing agent) is injected into the cavity to only partially fill the mold (realizing a so called "short shot"). Because of the sudden reduction of pressure the blowing agent expands and the foam fills the cavity.

To produce a foamed part with optimal properties, it is essential to optimize the injection molding processing parameters. The main variables involved are the amount of melt injected (namely the percentage of the cavity filled with the short shot), the mold and melt temperatures, the type and concentration of blowing agent, and the imposed flow rate. Some recent studies in the literature have dealt with the effect of various processing parameters like amount of gas, screw rotation speed, gate thickness, injection flow rate, melt temperature on the cell size, and cell density.[1–3]

The presence of gas inside the polymer can reduce its viscosity,[4,5] thus allowing the processability of the polymer at lower temperatures and pressures. This is an advantage particularly for biodegradable polymers, which are thermally sensitive and have narrow processing windows.[6] The increasing interest for biodegradable polymers has therefore further boosted the appeal of foam injection molding.[7] Among biodegradable polymers, polylactide (PLA) is the one that received most of attention by the researchers. However, it is very difficult to control the foaming of PLA by injection molding, because of its low melt strength and slow crystallization kinetics,[8–10] which makes it very challenging to achieve uniformly distributed fine-celled PLA foams with high void fractions.[11,12] For these reasons, just a few and quite recent studies on foam injection molding of PLA are available in the literature.

In a previous article[13] foaming of the same material adopted in this work was carried out, considering the effect of mold temperature, injection flow rate, and the addition of nucleating agents on the morphology of injection molded foamed parts was analyzed. In this work, another important process variable, namely the back pressure, was analyzed for the optimization of foam injection molding of PLA. Back pressure is the pressure imposed at the back of the screw when it is returning back to prepare a new amount of material to be injected (batching phase). In the batching phase, the polymer is loaded and the

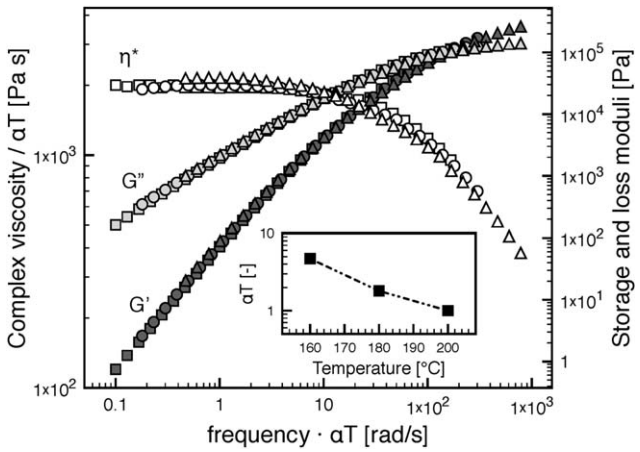

Figure 1. Rheological measurements on PLA Natureworks 4032D.

gas is simultaneously injected inside the cylinder. On increasing the back pressure, the batching time increases and thus also the mixing is longer. It is therefore expected that a higher back pressure allows a better gas dispersion inside the polymer melt.[14] Indeed, the back pressure also determines the amount of polymer conveyed from the cylinder toward the nozzle: a force balance sets in between the back pressure (which acts at the back of the screw), the friction along the screw and the pressure at the tip of the cavity which is given by the melt which accumulates in the injection chamber and, for the special case of foam injection molding, the gas injected. On decreasing the back pressure, the screw can be pushed back by the gas injected and the amount of polymer in the injection chamber can decrease. The study of the effect of back pressure is therefore nontrivial.

MATERIALS AND METHODS

A commercial grade of PLA produced by Natureworks with the trade name of 4032D with a D-enantiomer content of ~2% and with a maximum degree of crystallinity of about 45%[15] was adopted. PLA 4032D has a molecular weight distribution characterized by $M_n = 120$ kg/mole and $M_w = 210$ kg/mole. A rheological characterization of the material was carried out by a rotational rheometer in dynamic mode in parallel plates configuration. Figure 1 shows the results of rheological measurements, in terms of a master curve at $T = 200°C$. αT represents the thermal shift factor, whose values are reported in the insert of Figure 1.

A traditional injection molding machine (a 70 ton Negri-Bossi press) with screw diameter of 25 mm and $L/D = 22$ was adopted. Soon downstream from the shut-off nozzle, having a diameter of 2 mm, the sprue tapered from a diameter of 4,7 mm (at nozzle side) to a diameter of 7 mm (at mold side) over a length of 80 mm. The runner had a diameter of 8 mm and was 68 mm long. The material was injected into a line gated rectangular cavity of 120 mm × 30 mm × 4 mm (the latter dimension refers to cavity thickness). A gate with 0.5 mm of thickness and 6 mm of length was chosen, in order to have a maximum pressure drop at the cavity entrance thus reducing foaming inside the sprue and the runner.

The molding machine and the mold were equipped with four piezoelectric transducers for pressure measurement, which were located along the flow path: one just before the gate, and three in the cavity at 15 mm, 60 mm, and 105 mm from the gate. These positions will be referred to as P1, P2, P3, and P4, respectively. The pressures were acquired by a data acquisition system. A complete description of cavity geometry is reported in Figure 2.

The very narrow processing window of the PLA, due to the sensitivity to thermal degradation, restricts the injection temperature range at 180−220°C, while the relatively low glass transition temperature limits the mold temperature below 55−60°C.[16,17] Table I shows the experimental conditions adopted in this work.

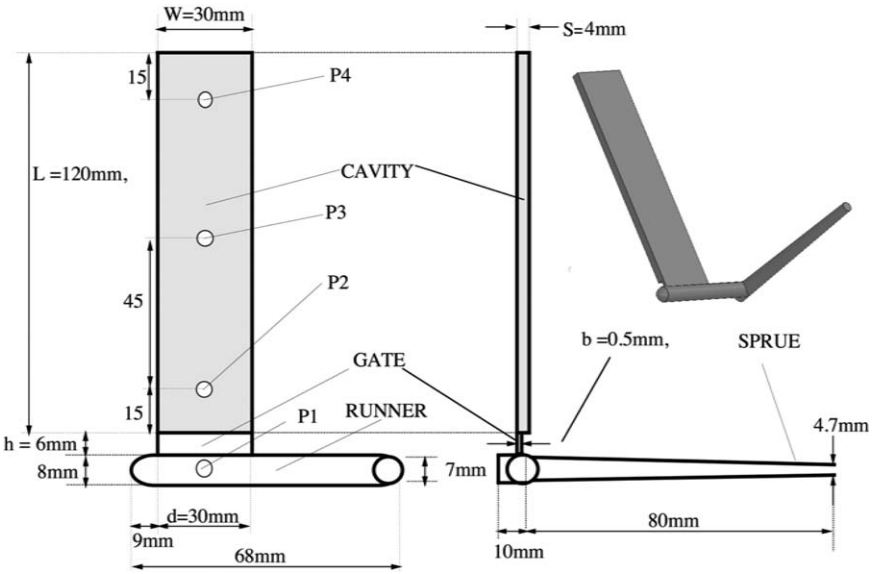

Figure 2. Schematic view of the cavity.

Table I. Experimental Conditions

Injection temperature (°C)	200
Gas pressure (bar)	0, 100
Injection flow rate (cm^3/s)	18
Rotation speed (rpm)	200
Shot volume supplied (cm^3)	27
Back pressure, bp (bar)	2–5
Mold temperature (°C)	25

A volumetric pump connected by an injector to the cylinder of the injection molding machine allows monitoring of the amount of gas injected during the batching step. Knowing the values of pressures and volumes before and after the injection of gas by means of the pump, the molar volume of nitrogen allows to obtain the numbers of moles injected and the corresponding amount in grams.

In this work, the effect of back pressure, bp, on the foamed parts was investigated. In particular, the length of batching and the pressure of the gas injected were kept constant and tuned so to obtain a complete part with a back pressure of 5 bar, whereas the back pressure was changed in the range from 2 bar to 5 bar. These values correspond to the back pressure in the hydraulic system. On the melt, the pressure was about 18 times larger.[18] Being the gas pressure 100 bar, it was not possible to inject gas with back pressures higher than 5 bar (corresponding to about 90 bar on the melt. It is important to note that the shot volume supplied must include not only the cavity volume, but also a scrap volume comprising sprue, runner, and gate.

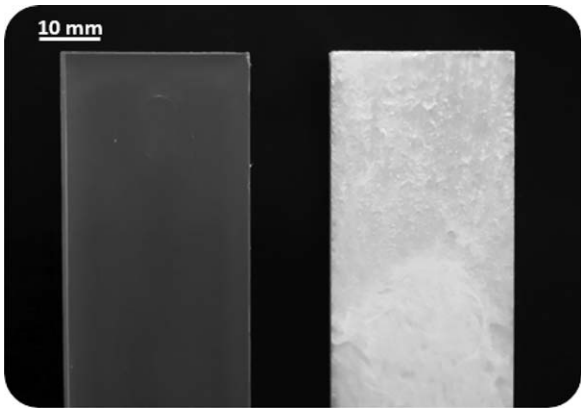

Figure 4. Comparison between an unfoamed (left) and a foamed part (right) obtained with a back pressure, bp, of 5 bar.

Density Measurements

Density measurements were performed at 25°C by weighing the samples immersed in water on the basis of Archimedes' principle. The measurements were carried out on the whole molded parts and on samples 10 mm long, cut horizontally at 10 mm and 80 mm from the gate, as shown in Figure 3(a). Density measurements will be expressed in terms of density reduction, R, with respect to the unfoamed part according to eq. (1), where ρ_0 is the density of the unfoamed PLA and ρ_f is the density of the foamed part.

$$R = \frac{\left(\rho_0 - \rho_f\right)}{\rho_0} \tag{1}$$

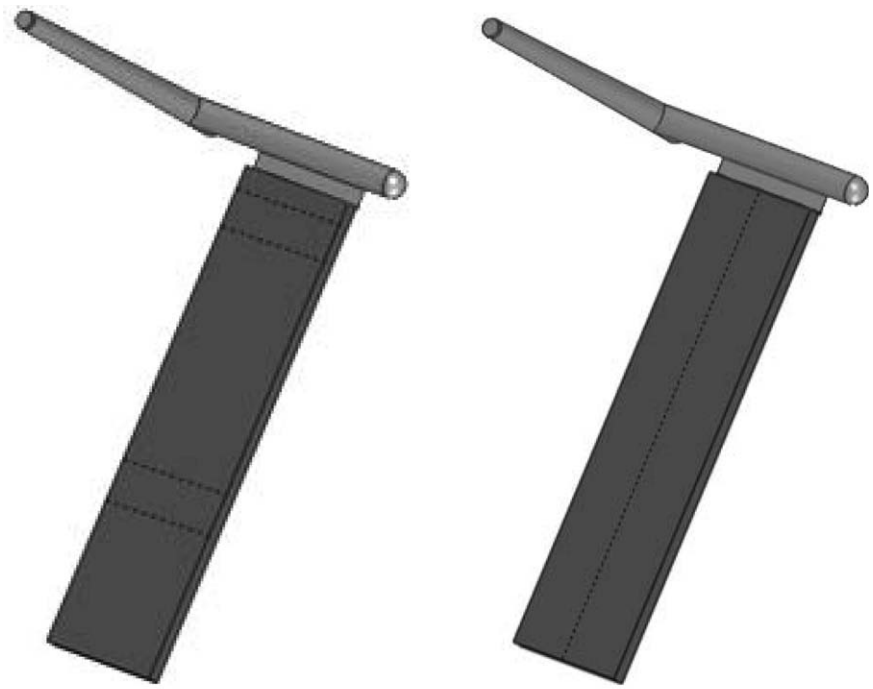

Figure 3. (a) Specimen cut at two positions along the flow path for density measurements; (b) specimen used for mechanical tests.

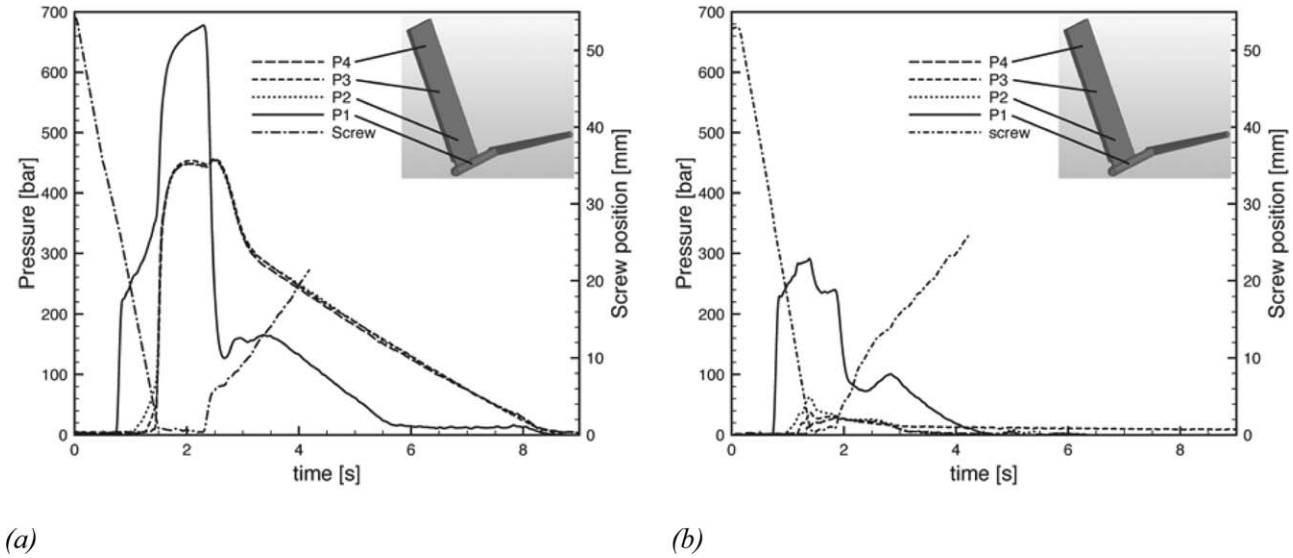

Figure 5. Pressure evolution measured during the injection molding test carried out: (a) without gas; (b) with gas and a back pressure of 5 bar.

Mechanical Tests

Samples for mechanical tests were cut vertically into two symmetric parts as shown in Figure 3(b). One of these parts was used for flexural test and the other part for tensile test.

Flexural tests were carried out by means of a universal testing machine mod ATSFAAR TC1000, with a load cell of 10 KN. The specimen was placed on two supports with a distance of 60 mm and loaded midway between the supports with a speed of 5 mm/min.

Tensile tests were performed by using the same machine. The test specimens were placed in the grips with a gage length of 60 mm and loaded at a speed of 10 mm/min until breaking.

A normalized modulus E_N was calculated as:

$$E_N = \frac{E_F}{E_0} \cdot \frac{\rho_0}{\rho_F} \quad (2)$$

where E_F is the Young's modulus of the foamed sample, E_0 is the Young's modulus of the unfoamed sample, ρ_0 is the density of the pure PLA, and ρ_F the density of the foamed PLA sample. The normalized modulus allows to keep into account the density reduction and the change of modulus.

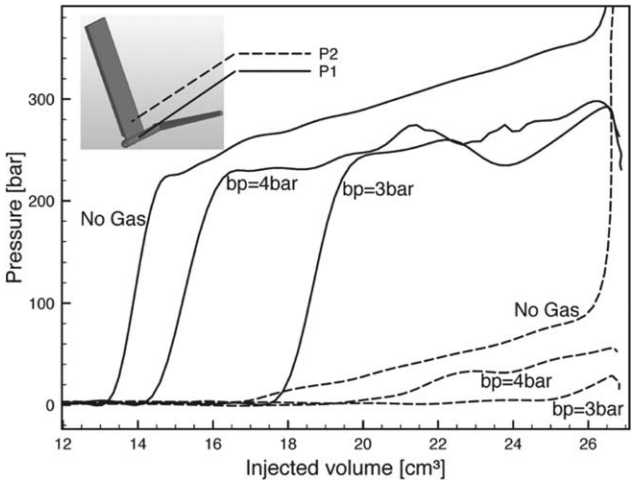

Figure 6. Pressure evolution in two positions versus the injected volume. "bp" stands for back pressure.

RESULTS

Injection Molding

In Figure 4 it is possible to observe the appearance of an unfoamed sample (left) and a foamed one, obtained with a bp of 5 bar (right). Samples obtained by traditional injection molding appear transparent and with a smooth surface. However, they present surface shrinkage marks, typical of injection-molded samples during the cooling phase in the absence of holding pressure. Samples obtained by foam injection molding keep perfectly the shape (no shrinkage during the cooling phase) even without holding phase. They appear white and opaque, with surface streaks representing the flow lines.

The pressure evolution measured during the injection molding tests carried out without gas injection are shown in Figure 5(a).

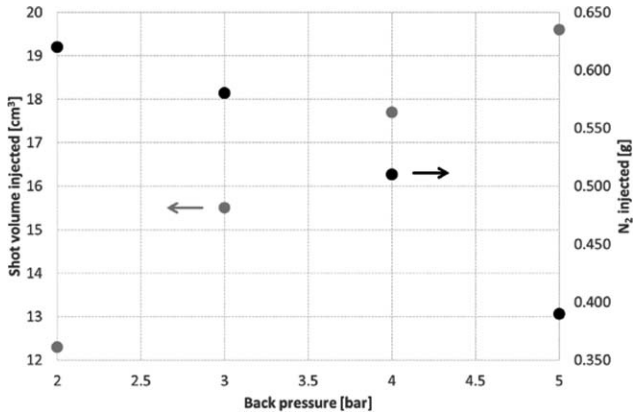

Figure 7. Volumes of N_2+PLA solution injected (measured at 1800 bar) for different back pressures (imposed by the hydraulic system) and grams of N_2 present in the volume.

Table II. Geometrical and Physical Features of the Foamed Samples of PLA 4032D at Different Back Pressures in the Hydraulic System

Back pressure (bar)	Amount of N_2 in PLA (g)	Length (mm)	Filled cavity volume (%)	Reduction in density (%)
2	0.62	91.22	76.0	25
3	0.58	98.09	81.7	27
4	0.51	112.15	93.5	15
5	0.39	120.00	100.0	12

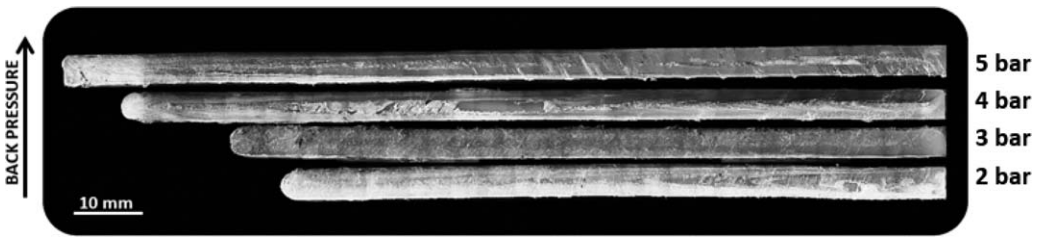

Figure 8. Vertical section of the foamed samples at different back pressures. The material flow direction is from right to left.

It can be noticed that, due to the presence of a thin gate and a relatively large cavity thickness, the pressure inside the cavity is homogenous. The filling phase lasted about 1.5 s, as evidenced by the screw position. Afterwards, the pressure soon before the gate keeps on increasing, mainly because of the large compressibility of the material, for about 0.7 s until the screws is moved back and the pressure in the channel soon drops down. Due to this pressure reduction upstream, also the pressure inside the cavity suddenly reduces because of backflow, namely some material leaves the cavity going back through the gate. After about 3 s from the start of filling the gate solidifies and the pressure curves inside the cavity start to decrease at a lower rate, essentially determined by the cooling. After 8 s, the pressure inside the cavity reaches zero and thus the polymer detaches from the cavity surface. The molded part is therefore smaller then the cavity. The part was demolded after 90 s.

The pressure profiles deeply change in the presence of gas. In Figure 5(b) the pressure profiles measured during the test conducted with a backpressure of 5 bar are reported. It is possible to notice that the pressure values are much lower everywhere, in spite of the fact that the cavity results completely filled at ejection. This is obviously due to the presence of gas which expands and compensates the thermal shrinkage.

As specified above, the back pressure also determines the amount of polymer conveyed toward the injection chamber during the batching phase. This means that on decreasing the back pressure, for the same injected volume (corresponding to set length of batching multiplied by the screw section) a lower mass of polymer is expected to be injected into the cavity. This completely changes the compressibility and the other physical properties of the injected mixture as evidenced by Figure 6, in which the measured pressure profiles in pos. P1 and P2 are reported versus the injected volume calculated by the screw position for some of the tests conducted in this work. The pressure at a given position starts to increase when the material reaches that position. Figure 6 demonstrates that the volume to

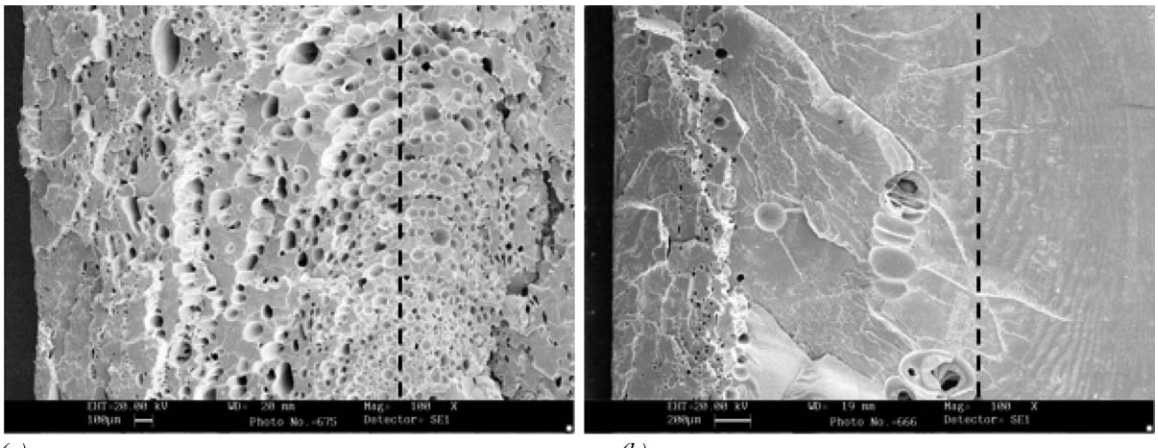

Figure 9. SEM micrographs of the section at 60 mm from the gate (flow/expansion direction toward the reader) of samples molded with back pressure 3 bar and 5 bar, respectively. The midplane is marked with dotted lines.

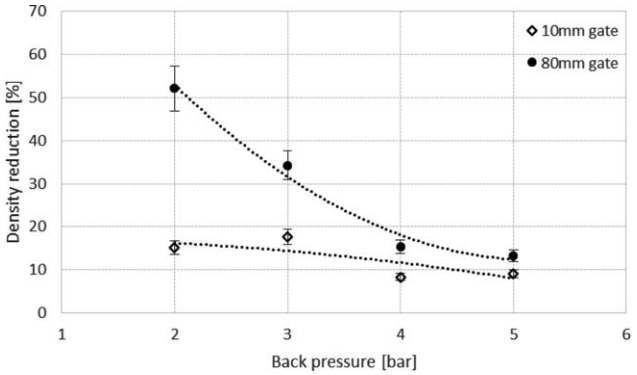

Figure 10. Density reduction of PLA 4032D at 10 mm and 80 mm from the gate, obtained with different back pressure.

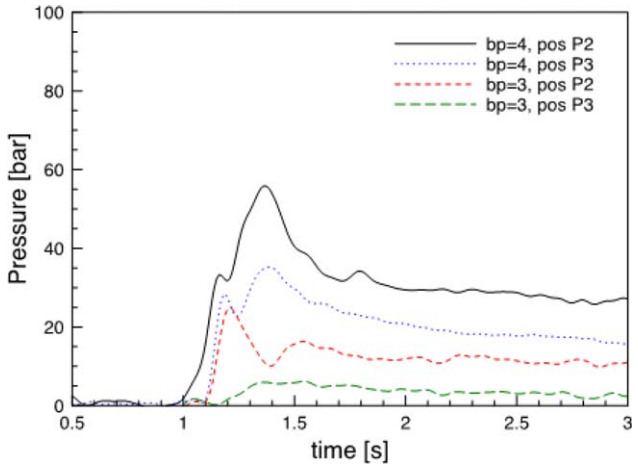

Figure 11. Pressure profiles measured for two different back pressures. [Color figure can be viewed in the online issue, which is available at wileyonlinelibrary.com.]

be injected in order to reach a given position increases on decreasing the back pressure. This clearly indicates a larger compressibility of the shot with a lower back pressure due to a larger amount of gas.

To better quantify this phenomenon, some tests were carried out by keeping the nozzle closed for some seconds while the pressure imposed by the screw was equal to 1800 bar. During these tests, the screw moved forward and the volume of the shot reduced from the initial (set) value to a value determined by the compressibility (which is essentially determined by the amount of polymer). The screw position was monitored and this allowed to compare the volumes of the injected shots for the same pressure and temperature. The volumes are reported in Figure 7 together with the grams of N_2 injected for each conditions (determined by the volumetric pump).

It can be observed that at higher values of back pressure a larger quantity of PLA-N_2 mixture and a lower value of N_2 are injected. The lower amount of gas is determined by the smaller difference between the pressure in the cylinder during the gas injection and the gas pressure. On increasing the back pressure, the batching time increases and the mixing is probably more efficient, but the percentage of foaming agent inside the injection chamber is smaller as also reported in Table II. It is therefore expected that the foaming is more effective for lower values of back pressure. However, due to the poorer mixing, not all the injected gas takes part to the foaming process, and therefore the volume of the injected part is smaller.

Table II also reports the length of the samples, the filled cavity volume, namely the ratio between the cavity volume filled by the injected polymer and the cavity volume (14.4 cm^3), and the density reduction with respect to the unfoamed samples. On increasing the back pressure, samples are longer and have higher density.

Figure 8 shows a length-thickness section of foamed samples at increasing bp from the bottom upwards. As stated previously, sample length increases with the bp and only the sample obtained with a bp of 5 bar results to be complete.

In samples obtained with back pressures of 4 and 5 bar, foaming mostly occurs at the tip of the part. For most of the sample length, just regions close to the midplane present voids, whereas a significant layer close to the sample skin is completely unfoamed. The samples obtained with a bp of 4bar, in particular, show very large voids, having a characteristic dimension of more than 1 mm, in the core region. The morphology is different for samples obtained with back pressures of 2 and 3 bars.

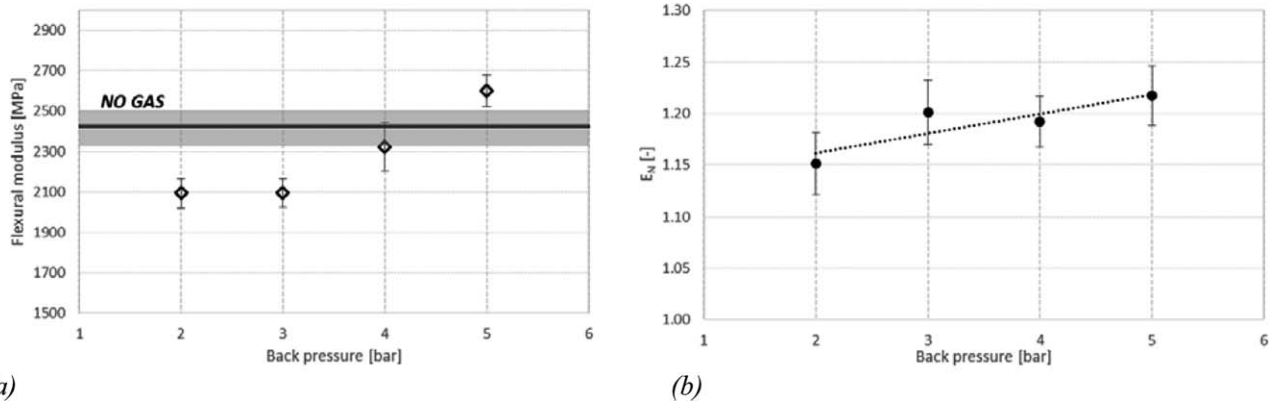

Figure 12. (a) Modules of elasticity obtained by flexural tests at 5 mm/min for PLA 4032D samples foamed with different back pressure; line represents the average value of the flexural modulus of samples without gas; (b) normalized modulus of elasticity.

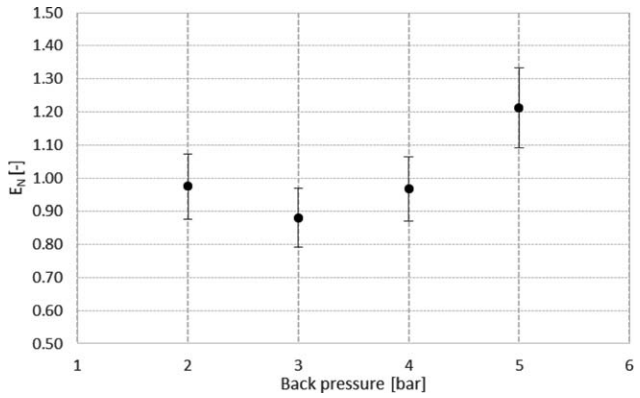

Figure 13. Normalized modulus of elasticity obtained from tensile tests at different back pressures.

In these cases, foaming is more homogeneous in the whole sample, even if at regions closer to the gate a significant unfoamed skin layer exists, with just some large voids (having characteristic dimension of the order of 100 μm) at sample core.

Figure 9(a,b) show SEM micrographs of the half-thickness section at 60 mm from the gate (flow/expansion direction toward the reader) of samples molded with back pressure 3 bar and 5 bar, respectively.

As it is possible to observe, sample molded with bp = 3 bar shows compact skin thickness lightly smaller than that of the sample molded with bp = 5 bar. A significant difference between the morphologies of the two samples is in the remaining part. This area can be divided in two zones: the transition layer, which begins at the end of the skin layer, and the core region, which lies in the middle of the sample. The samples molded with bp = 3 bar shows a large transition layer (about 1 mm thick), consisting in cells with size in the range 50−150 μm surrounded by compact zones, and a core region consisting in a great number of small cells (smaller than 100 μm). The sample molded at 5 bar shows a small transition zone (about 300 μm) and a core region consisting in a large compact zone and a few cells with diameter higher than 150 μm.

As observed above, the morphology of the samples is not homogeneous along the length direction. As a consequence, the density reduction is also not homogenous. Density measurements were carried out on specimens taken at two positions along the flow path [Figure 3(a)] and the results are reported in Figure 10. A large difference in density exists between the part closer to the gate and the part at 80 mm from the gate. This is due to the pressure inside the cavity which, as shown in Figure 11, increases on increasing the back pressure and inhibits the foaming.

Mechanical Properties

Figure 12(a) shows the flexural modulus measured on the analyzed specimens.

With increasing back pressure, it can be observed an initial reduction in modulus with respect to the modulus of the unfoamed part, and a subsequent increase at high bp. If the modulus is normalized by eq. (2), values larger than 1 are found [Figure 12(b)]. This means that the decrease in modulus is less relevant than the decrease in density.

Figure 13 reports the modulus of elasticity obtained from tensile tests at different back pressures. In this case, measurements provided values of normalized modulus smaller than 1 for all back pressures except the largest one (5 bar). The difference in behavior between tensile and flexural moduli are due to the inhomogeneous foaming of the samples along the thickness direction.[19] The unfoamed skin layer, which deforms more during flexural tests, essentially determines the mechanical properties for that kind of solicitation. The core region, more foamed, is located instead close to the neutral axis. On the other hand, tensile tests solicit the whole section of the specimen and thus the measured properties are poorer, especially in the presence of large cells.[20,21]

The tensile strength, reported in Figure 14(a), shows a minimum in correspondence of bp equal to 3 bar. The strain at break [Figure 14(b)] shows a decreasing trend with the bp, essentially following the general trend of density reduction.

CONCLUSIONS

Foam injection molding of a commercial grade PLA was carried out by a traditional injection molding machine, modified only in the cylinder to allow the gas injection. The effect of back pressure on the batching phase and on the foamed part was

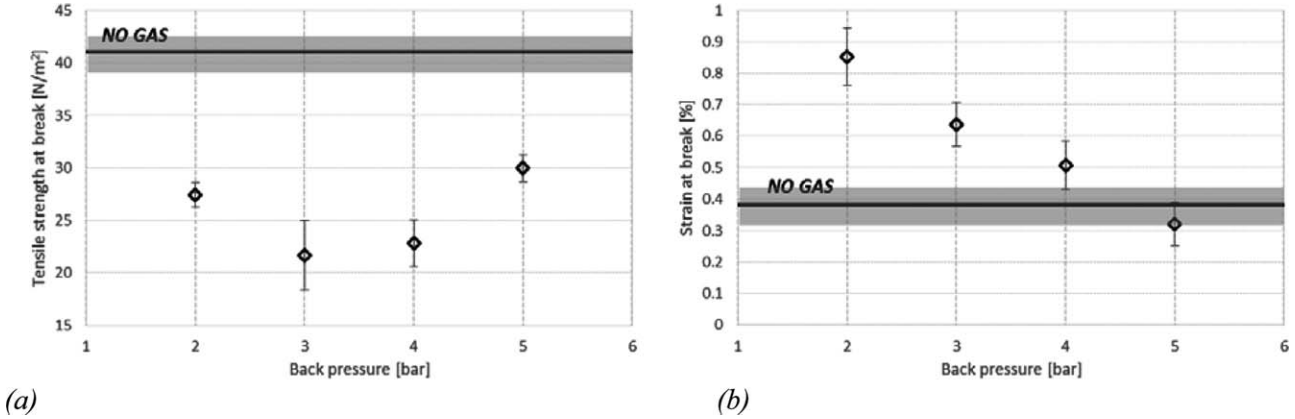

Figure 14. Tensile strength at break (a) and strain at break (b) of PLA 4032D foamed part at different back pressures and the unfoamed part.

analyzed, keeping constant the length of batching and the pressure of the gas injected. In particular, the back pressure was changed in the range 2–5 bar in the hydraulic system corresponding to about 35−90 bar on the melt. On the basis of the experimental observation carried out, it could be concluded that:

- On decreasing the back pressure, a lower amount of polymer is injected due to the fact that the gas pushes back the screw reducing the conveying of polymer toward the injection chamber. The resulting samples are therefore shorter but more foamed, with density reductions as high as 25%.
- Foaming improves going from the gate to the tip of the part, due to the smaller pressures reached which enable foaming.
- Flexural tests provided values of normalized modulus larger than 1, meaning that the density reduction marginally affects the value of the modulus. This happens because the unfoamed skin layer determines the mechanical properties during flexion.
- Tensile measurements provided instead values of normalized modulus smaller than 1 for all back pressures except the largest one (5 bar). This happens because the presence of large voids in the foamed specimens reduces the effective load bearing area, resulting in tensile strength and Young's modulus of the microcellular specimens lower than that of their solid counterparts.

REFERENCES

1. Pantani, R.; Sorrentino, A.; Volpe, V.; Titomanlio, G. *AIP Conf. Proc.* **2014**, *1593*, 397.
2. Lee, J. W. S.; Wang, J.; Yoon, J. D.; Park, C. B. *Ind. Eng. Chem. Res.* **2008**, *47*, 9457.
3. Lee, J. J.; Turng, L. S.; Dougherty, E.; Gorton, P. *Polymer* **2011**, *52*, 1436.
4. Areerat, S.; Nagata, T.; Ohshima, M. *Polym. Eng. Sci.* **2002**, *42*, 2234.
5. Choudhary, M.; Delaviz, Y.; Loh, R.; Polasky, M.; Wan, C.; Todd, D. B.; Hyun, K. S.; Dey, S.; Wu, F. *J. Cell. Plast.* **2005**, *41*, 589.
6. Speranza, V.; De Meo, A.; Pantani, R. *Polym. Degrad. Stab.* **2014**, *100*, 37.
7. Jeon, B.; Kim, H. K.; Cha, S. W.; Lee, S. J.; Han, M. S.; Lee, K. S. *Int. J. Precis. Eng. Man.* **2013**, *14*, 679.
8. Liao, X.; Nawaby, A. V.; Naguib, H. E. *J. Appl. Polym. Sci.* **2012**, *124*, 585.
9. Xiao, H. W.; Li, P.; Ren, X. M.; Jiang, T.; Yeh, J. T. *J. Appl. Polym. Sci.* **2010**, *118*, 3558.
10. Pantani, R.; De Santis, F.; Sorrentino, A.; De Maio, F.; Titomanlio, G. *Polym. Degrad. Stab.* **2010**, *95*, 1148.
11. Nofar, M.; Park, C. B. *Prog. Polym. Sci.* **2014**, *39*, 1721.
12. Ameli, A.; Jahani, D.; Nofar, M.; Jung, P. U.; Park, C. B. *J. Cell. Plast.* **2013**, *49*, 351.
13. Pantani, R.; Volpe, V.; Titomanlio, G. *J. Mater. Process. Technol.* **2014**, *214*, 3098.
14. Rizvi, S. J. A.; Bhatnagar, N. *Int. Polym. Proc.* **2009**, *24*, 399.
15. Gorrasi, G.; Pantani, R. *Polym. Degrad. Stab.* **2013**, *98*, 1006.
16. Taubner, V.; Shishoo, R. *J. Appl. Polym. Sci.* **2001**, *79*, 2128.
17. Bhatia, A.; Gupta, R. K.; Bhattacharya, S. N.; Choi, H. J. *J. Appl. Polym. Sci.* **2009**, *114*, 2837.
18. Speranza, V.; Vietri, U.; Pantani, R. *Macromol. Res.* **2011**, *19*, 542.
19. Xu, J.; Kishbaugh, L. *J. Cell. Plast.* **2003**, *39*, 29.
20. Zhao, H. B.; Cui, Z. X.; Wang, X. F.; Turng, L. S.; Peng, X. F. *Compos. Part B-Eng.* **2013**, *51*, 79.
21. Pilla, S.; Kramschuster, A.; Lee, J.; Clemons, C.; Gong, S. Q.; Turng, L. S. *J. Mater. Sci.* **2010**, *45*, 2732.